ATLANTIS PRESS

Advances in Computer Science Research, volume 93

2nd International Conference on Mathematics, Modeling and Simulation Technologies and Applications (MMSTA 2019)

Thermal Characteristic on Ranging Arm Shell of Drum Shearer

Xiangkun Song*, Ruiguang Yun, Chunxiang Shi and Changfei Zhou
Shanghai Branch of Tiandi Science & Technology Co, Ltd, China
*Corresponding author

***Abstract*—Aiming at the problem of shear damage of shearer ranging arm caused by thermal load and force load, the ranging arm shell of the drum shearer is taken as research object, the mechanical properties, temperature field distribution and thermal characteristics of the ranging arm shell are carried out. Based on the theory of heat transfer, the heat generation and heat dissipation of the ranging arm are analyzed, the heat balance analysis of the ranging arm shell is built, and the heat balance temperature at different environment temperatures is calculated. The thermal analysis and thermal structure coupling analysis of the arm shell are carried out, and the stress and deformation distribution of the ranging arm shell are obtained. The results shows that the maximum stress and maximum deformation of the ranging shell are greatly increased under the thermal balance temperature. The correctness of the thermal analysis method is verified by the loading experiment.**

Keywords—ranging arm; heat balance; thermal analysis; thermal structure 批

I. INTRODUCTION

The drum shearer ranging arm is an important part of the power transmission system. The ranging structure of the drum shearer is shown in Figure 1. The strength, stiffness and thermal characteristics of the ranging arm shell have a significant influence on the transmission performance. When the ranging arm shell is subjected to heavy load, under the combined action of heat and force, defects such as cracking or excessive deformation may occurs in the weak part, which will greatly affect the transmission effect and dynamic performance of the bearing and gear in the ranging arm. Consequently, the arm shell and transmission system may face many thermal and mechanical problems.

The existing research contents of shearer mainly include: Gao[1] analyzed the torsional vibration transmission process of the shearer drive shaft, theoretically derived the torsional vibration equation of the shaft. Si[2] made use of the vibration characteristics of ranging arm, proposed a diagnosis method of shearer cutting state based on PNN and FOA. Yang[3] compared the vibration signal with the shearer in a healthy state by vibration analysis method, to conduct fault diagnosis. Xu[4] established a shearer adaptive memory cutting model based on fuzzy control theory, which can well meet the control requirements under complex geological conditions. Wang[5] analyzed the statics force of the shearer drum and optimized the design of the shell. Lian[6] established a virtual prototype of the shearer ranging arm and analyzed the dynamics characteristics of the ranging arm. Zhang[7] analyzed the nonlinear dynamic characteristics of the ranging arm drive system. From the reliability point of view, used the fourth-order matrix method to optimize the reliability of the system. Mao[8]carried out the thermal coupling analysis of the ranging arm gear, and modified the tooth profile on the basis of analysis. Chen[9]took the shearer gear pair as the research object, the three-degree-of-freedom nonlinear dynamic model of the gear pair was established, and the dynamic characteristics of the system were analyzed, the systemic chaos was well suppressed with the periodic resonance excitation method. Chen[10] established the solid-heat-force coupling characteristic model of the shearer gear transmission system, and studied the heat generation characteristics of the idler gear under different ambient temperatures. In existing research, most focus on the shearer drum and transmission gear, there is less analysis of the thermal characteristics of the ranging arm of the drum shearer.

This paper has studied the mechanical properties, temperature field distribution and thermal characteristics of the ranging arm shell of the drum shearer, analyzes the heat generation and heat dissipation factors of the ranging arm. On this basis, the heat balance model of the ranging shell is built. Then the thermal analysis and thermal structure coupling analysis of the ranging arm shell is carried out. Finally, the loading experiment verifies the correctness of the thermal analysis method.

1-truncture four-axis assembly; 2-idual two-axis assembly; 3-cut three-axis assembly; 4-cut two-axis assembly; 5-pilot one-axis assembly; 6-to-one shaft assembly; 7-miner drum

FIGURE I. SHEARER RANGING ARM

II. THE RANGING ARM HEAT GENERATION AND HEAT DISSIPATION ANALYSIS

A. Heat Generation Analysis

The heat generated by the ranging arm mainly caused by mechanical friction and oil churning friction. Among them, the mechanical friction includes the gear friction and the bearing friction, and the oil churning friction mainly refers to the gear oil churning and the bearing oil churning. Friction finally converted into heat, which causes the oil temperature to rise, the viscosity of the oil to decrease, and the oil film to fail or the bearing capacity to decrease, which will cause serious damage to the gears, bearings and other components. Consequently, the temperature rise has a great impact on the stress and deformation of the ranging arm, and then affects the overall operational reliability of the ranging arm.

1) Gear meshing heat: During the gear meshing process, sliding friction occurs due to the relative sliding between the two tooth surfaces that press against each other, and then friction heat generates on the meshing surface. The gear meshing power is the heat generating power, the meshing loss power includes sliding friction Power and rolling friction power. The sliding friction power loss can be calculated using equations (1) and (2) [11].

$$P_s = q_s L_s B_c \tag{1}$$

$$q_s = f_s p_s V_s \tag{2}$$

where, P_s is the gear sliding friction power loss, q_s is the heat flux density of the tooth surface sliding friction, L_s is the gear mesh length, B_c is the gear width; f_s is the sliding friction coefficient, p_s is the tooth surface contact stress at the meshing point, V_s is the relative sliding speed meshed for the gears.

The rolling friction power loss of the gear is calculated according to the relative rolling model of the cylinder. The calculation method is:

$$P_r = 9000 \cdot \frac{bV_r h\varepsilon}{\cos\beta_b} \tag{3}$$

$$V_r = 0.2094 n_1 \left(r_1 \sin\alpha - 0.125 L \frac{z_2 - z_1}{z_2} \right) \tag{4}$$

$$L_s = \sqrt{r_{a1}^2 - r_1^2 \cos^2\alpha} + \sqrt{r_{a2}^2 - r_2^2 \cos^2\alpha} - (r_1 + r_2)\sin\alpha \tag{5}$$

$$h_{oil} = 2.051 \times 10^{-7} \left(\eta_e V_r\right)^{0.067} F_n^{-0.067} \rho^{0.046} \tag{6}$$

where, V_r is the average relative rolling speed, L_s is the meshing line length, h_{oil} is the oil film thickness; ε is the gear meshing coincidence degree, β_b is the driving gear base circular helix angle, and the spur gear base circular helix angle β_b=0°, m is Gear modulus, ρ is the density of the lubricant.

2) Bearing heat: Bearing heat production power is mainly derived from friction and bearing oil[12]. Because the ranging arm is subjected to heavy load during its working time, its transmission system mainly uses cylindrical roller bearings, tapered roller bearings and spherical roller bearings. Therefore, only these three are considered when analyzes the heat generation of ranging arm bearings.

The calculation formula for bearing heat is:

$$P_z = \frac{\pi n M}{60} \times 10^{-3} \tag{7}$$

where, P_z is the bearing power loss, M is the total friction torque of the bearing, N is the bearing speed.

3) Gear oil churning heat: Gear churns oil to produce heat, which will cause the temperature of gear and lubricant to rise and the transmission efficiency of the system to decrease. The Gear oil churning heat is the power lost by oil churning. The factors affect gear oil churning heat include gear geometry, gear speed, gear oil immersion depth, lubricant temperature and ranging arm chamber size[13]. In this paper, BS ISO/TR14179 [14] standard is used to calculate the power of gear oil churning. The power of gear oil churning is divided into three parts: the power between gear shaft and oil, the power between gear side and oil, and the power between gear circumference and oil.

The power between gear shaft and oil:

$$P_{c1} = \frac{7.37 h_g \nu n^3 D_a^{4.7} L}{0.2 \times 10^{26}} \tag{8}$$

The power between gear side and oil:

$$P_{c2} = \frac{1.474 h_g \nu n^3 D_a^{5.7}}{0.2 \times 10^{26}} \tag{9}$$

The power between gear circumference and oil

$$P_{c3} = \frac{17.547 h_g \nu n^3 D_a^{4.7} B R_f}{0.2 \times 10^{26}} \tag{10}$$

$$R_f = \frac{R_{f1} + R_{f2}}{2} \sqrt[3]{\frac{100}{a}} \tag{11}$$

where, D_a is the diameter of gear tip circle, B_c is the tooth width, L is the shaft length, v is the oil kinematic viscosity, n is the gear rotation speed, R_f is the gear roughness factor, R_{f1} and R_{f2} are the meshing gear coarseness respectively Degree, a is the center distance of the two gears, h_g is the gear immersion scale factor, when the gear is not immersed in the oil, h_g=0, when the gear is completely immersed in the oil, h_g=1.

B. Heat Dissipation Analysis

The drum shearer ranging arm usually dissipates heat in three ways, namely through the shell wall and the air convection heat transfer, the ranging cooling spray system heat dissipation and the lubricating oil heat absorption.

1) The heat dissipation process of ranging arm shell: The heat dissipation process of ranging arm shell wall is: high temperature lubricating oil convection with the inner wall of the shell, heat transfers from the inner wall to the outer wall of the shell, and heat convection between the outer wall of the shell and the flowing air.

The heat dissipation of ranging arm shell wall is calculate according to Newton cooling formula[15]:

$$\phi_S = hS\Delta t \tag{12}$$

where, ϕ_S is convective heat transfer heat, h is convective heat transfer coefficient, S is convective heat transfer area, Δt is the temperature difference between the heat transfer surface and the fluid.

2) The ranging arm cooling system: The ranging arm cooling system is divided into a forced water cooling system inside the ranging arm and an external spray cooling system. The two cooling systems have the same cooling mechanism and cool by water medium. The forced cooling system inside the ranging arm dips the circulating water cooler into the lubricating oil. The external spray system cooling water flows through the outer wall and the cylindrical surface, absorbs the heat on the surface of the shell, and the calculating formula as follows[16]:

$$\phi_w = c_w m_w \Delta t_w \tag{13}$$

Where, ϕ_w is the heat absorption of the cooler, c_w is the specific heat capacity of water, m_w is the quality of water passing through in unit time, Δt_w is the temperature difference between the outlet and the inlet of the cooling system.

3) The lubricating oil heat absorption: Shearer uses oil bath splash lubrication, lubricating oil and gas fill the whole ranging chamber. Lubricating oil exchanges heat with gears, bearings, etc. to absorb heat. At the same time, lubricating oil exchanges heat with ranging shell and cooler to dissipate heat, but heat generation is more than heat dissipation, so the temperature of oil increases. The heat absorption formula of lubricating oil is[17]:

$$Q_{oil} + Q_{mat} = cm_g \Delta t_{oil} + C_0 M_g \Delta t_{mat} \tag{14}$$

Where, Q_{oil} and Q_{mat} are heat of internal mechanism of oil and shearer ranging respectively, c and C_0 are heat capacity of internal mechanism of oil and shearer ranging arm respectively, m_g and M_g are mass of internal mechanism of lubricating oil and shearer ranging respectively.

III. THERMAL BALANCE ANALYSIS OF RANGING ARM

The thermal balance temperature of the ranging arm can be obtained by thermal balance analysis. It is found that the analysis of the stress and deformation caused by thermal load makes a great significance for improving the heat dissipation system of the ranging arm and prolonging the service life of the ranging arm. Because there are many components involved in heat generation and heat dissipation, and there are fluid media, the heat transfer relationship is complex. In order to analyze the heat balance of ranging arm more accurately, the thermal network method can be used. The heat transfer process inside the ranging arm is that heat generates by gear, bearing and churning oil, there is thermal resistance between each component and lubricating oil, and heat is transferred through thermal resistance. The heat in the lubricating oil and the structure include three parts, which are self-absorption to raise the body temperature, transmission to the ranging shell to diffuse into the air, and transmission from the lubricating oil to the cooler. The heat transfer process is shown in Figure 2. When the heat production and heat dissipation are the same, the system reaches the state of heat balance[18].

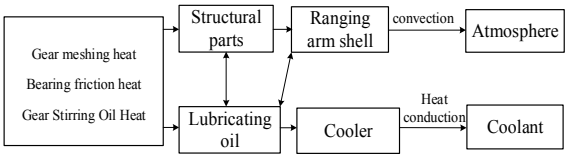

FIGURE II. HEAT TRANSMISSION DIAGRAM

A. Establishment of Thermal Network Model

It is necessary to construct a heat balance network model for thermal balance analysis of ranging arm by using thermal network method. In order to simplify the physical model of the ranging arm transmission system, the location of heat source and temperature nodes are determined, and the mechanical transmission system model of shearer ranging arm is converted into thermal network model of ranging arm thermal balance by using the heat resistance and heat transfer relationship between temperature nodes.

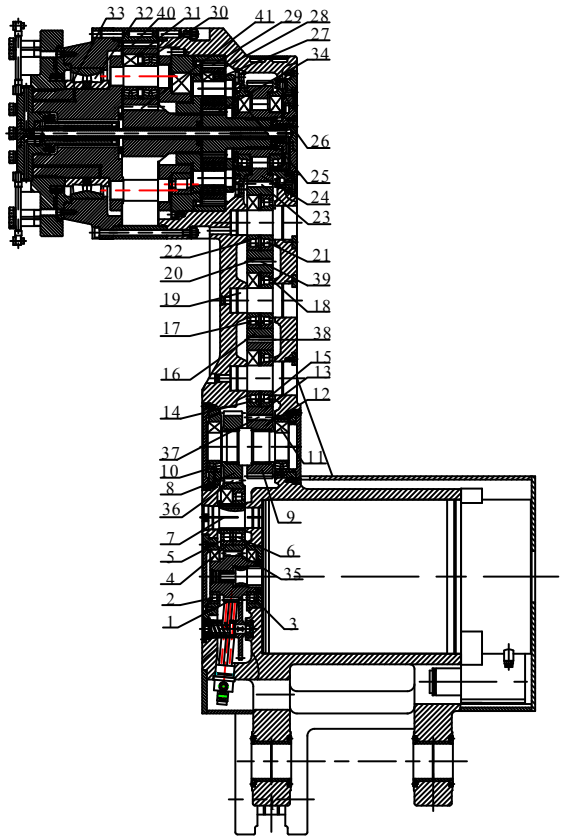

FIGURE III. SCHEMATIC DIAGRAM OF TEMPERATURE NODES ON SHEARER RANGING ARM

According to the heat transfer diagram, temperature nodes as shown in Figure 3, and the corresponding thermal network model shows in Figure 4. the thermal resistance between components is expressed as R_{ivj}, subscript *i* represents the node with higher temperature, *j* represents the node with lower temperature, gear meshing thermal resistance is expressed as R_{iSj}, subscript *i* represents the node with high speed axle gear, *j* represents the node with low speed gear, and label ⊗ represents the heat source.

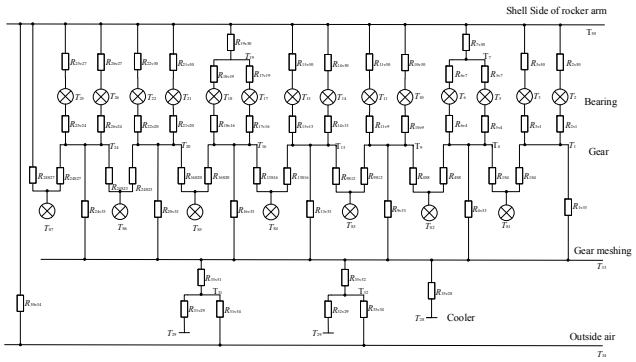

FIGURE IV. THERMAL NETWORK OF SHEARER RANGING ARM

B. Thermal Resistance between Ranging Arm Parts

Calculating the thermal resistance between the components of the ranging arm is a necessary condition for the analysis of the thermal balance of the ranging arm. In the analysis of ranging arm thermal balance, there are mainly four kinds of thermal resistance, i.e. gear meshing thermal resistance, oil mixing and non-oil mixing thermal resistance between gear and lubricant, shaft and bearing and thermal resistance between bearing and the shell, shell internal and external surface and external environment thermal resistance[16].

1) Gear meshing thermal resistance: A lot of heat generates during gear meshing, and there is thermal resistance in the process of heat transfer from gear meshing surface to gear body:

$$R_{cc} = \frac{0.767\xi}{\sqrt{l_h} \cdot B_z k \cdot \sqrt{v}} \tag{15}$$

where, R_{cc} is the thermal resistance of gear meshing, ξ is the thermal diffusivity of lubricating oil, l_h is the relative sliding speed of two gear meshing points, B_z is the tooth width, k is the heat transfer coefficient of gear material, v is the linear velocity of the point on the gear indexing circle.

2) Thermal Resistance between Stirred and Non-Stirred Gears and Lubricating Oil: In the process of ranging arm working, the oil-churning gear is immersed in lubricating oil, and the non-oil-churning gear is exposed to lubricating oil and gas.

When the gear is immersed in lubricating oil, the thermal resistance between the gear and lubricating oil depends on the dimensionless parameter ψ . The formula are as follows:

$$\psi = \left(D\xi \left(\pi - \xi \cos\left(\frac{2D_h - 2D_0}{mz} \right) \right)^2 \Big/ 2\upsilon h \right)^{\frac{1}{4}} \tag{16}$$

$$R_{cy} = \begin{cases} \dfrac{2\pi\sqrt{\xi}}{1.14 B_z \cdot 2z \cdot h \cdot w \cdot \sqrt{\tau}} & \psi \le 0.68 \\ \dfrac{2\pi\sqrt{\xi}}{(1.55 - 0.6\psi) B_z \cdot 2z \cdot h \cdot w \cdot \sqrt{\tau}} & 0.68 < \psi < 1.5 \end{cases} \tag{17}$$

where, R_{cy} is the thermal resistance of gear oil churning, D is the diameter of gear indexing circle, B_z is the tooth width. h is the tooth height, D_h is the distance from the axis to the bottom of the shell , D_0 is the depth of lubricating oil, ξ is the thermal diffusivity of lubricating oil, τ is the time from the oil surface to the beginning of meshing, ω is the angular velocity of gear, υ is the motion viscosity of lubricating oil.

When the gear is placed in both the oil and gas, the heat resistance of the gear is as follows:

$$R_{cq}=\frac{D}{0.133\lambda}\cdot\left(\frac{2}{\omega D^2}\right)^{\frac{2}{3}}\cdot(\xi\upsilon)^{\frac{1}{3}}\cdot\frac{1}{2S} \tag{18}$$

where, R_{cq} is the thermal resistance of gear stirring oil, D is the diameter of indexing circle, λ is the thermal conductivity of lubricating oil, ω is the angular velocity of gear, ζ is the kinematic viscosity of lubricating oil, υ is the kinematic viscosity of lubricating oil; S is the lateral area of gear.

3) Thermal Resistance Between Shaft and Bearing and Bearing and Shell: Shafts and bearings are regarded as temperature nodes. When calculating thermal resistance, shafts and bearings are regarded as cylinders. Their thermal resistance is as follows:

$$R_{zz}=\frac{\ln(R_o/R_i)}{2\pi\cdot k\cdot L} \tag{19}$$

where, R_{zz} is the thermal resistance of the shaft and bearing, R_o is the inner diameter of the part, R_i is the outer diameter of the part, k is the thermal conductivity of the part, L is the axial length of the part.

4) Thermal Resistance between Outer Surface of Shell and External Environment:

$$R_{kt}=\frac{l}{k_d\lambda}\cdot\left(\frac{\upsilon^2}{g\cdot\beta\cdot\Delta t\cdot l^3}\cdot\frac{\lambda}{\eta\cdot C_p}\right)^{0.30}\cdot\frac{1}{S} \tag{20}$$

where, R_{kt} is the thermal resistance between the shell surface and the environment, l is the characteristic size of the shell surface, λ is the thermal conductivity of lubricating oil, υ is the kinetic viscosity of lubricating oil, g is the acceleration of gravity, β is air expansion coefficient, Δt is the temperature difference between the shell surface and the external air; υ is the kinetic viscosity of lubricating oil, η is the aerodynamic viscosity, C_p is the air, Specific heat capacity at constant pressure, when calculating the upper and lower walls of the shell k_d=0.2, when calculating the side of the shell k_d=0.28, S is the surface area of the shell.

5) Thermal Resistance between Shell and Lubricating Oil:

$$R=\frac{1}{h_1 S} \tag{21}$$

where, h_1 is the convective heat transfer coefficient between the fluid inside the shell and the shell, S is the heat transfer area of the shell.

C. Establishment of Heat Balance Equation

In electricity, according to Kirchhoff's law, the inflow and outflow currents of any node in the circuit are equal. Extending this law to thermodynamics, it can be seen that when the heat transfer system reaches the heat balance, the inflow and outflow heat of any node are equal. According to this law, combined with the heat network of shearer ranging As is shown in Figure 4, the heat balance equation can be established for each temperature node, thus constituting the heat balance equation system of shearer ranging [17-18]:

$$(T_2-T_1)/R_{2v1}+(T_3-T_1)/R_{3v1}+(T_{S1}-T_1)/R_{1S4}=(T_1-T_{33})/R_{1v33}$$
$$P_2=(T_2-T_{30})/R_{2v30}+(T_2-T_1)/R_{2v1}$$
$$P_3=(T_3-T_{30})/R_{3v30}+(T_3-T_1)/R_{3v1}$$

$$(T_5-T_4)/R_{5v4}+(T_6-T_4)/R_{6v4}+(T_{S1}-T_1)/R_{1S4}+(T_{S2}-T_4)/R_{4S8}=(T_4-T_{33})/R_{4v33}$$
$$P_5=(T_5-T_7)/R_{5v7}+(T_5-T_4)/R_{5v4}$$
$$P_6=(T_6-T_7)/R_{6v7}+(T_6-T_4)/R_{6v4}$$
$$(T_6-T_7)/R_{6v7}+(T_5-T_7)/R_{5v7}=(T_7-T_{30})/R_{7v30}$$
$$T_8-T_9=0$$
$$P_{10}=(T_5-T_7)/R_{5v7}+(T_5-T_4)/R_{5v4}$$
$$P_{11}=(T_{11}-T_{30})/R_{11v30}+(T_{11}-T_9)/R_{11v9}$$
$$T_{12}-T_{13}=0$$
$$(T_{14}-T_{13})/R_{14v13}+(T_{15}-T_{13})/R_{15v13}+(T_{S3}-T_{13})/R_{9S12}+(T_{S4}-T_{13})/R_{13S16}=(T_{13}-T_{33})/R_{13v33}$$
$$P_{14}=(T_{14}-T_{30})/R_{14v30}+(T_{14}-T_{13})/R_{14v13}$$
$$P_{15}=(T_{15}-T_{30})/R_{15v30}+(T_{15}-T_{13})/R_{15v13}$$
$$(T_{17}-T_{16})/R_{17v16}+(T_{18}-T_{16})/R_{18v16}+(T_{S4}-T_{16})/R_{13S16}+(T_{S5}-T_{16})/R_{16S20}=(T_{16}-T_{33})/R_{16v33}$$
$$P_{17}=(T_{17}-T_{19})/R_{17v19}+(T_{17}-T_{16})/R_{17v16}$$
$$P_{18}=(T_{18}-T_{19})/R_{18v19}+(T_{18}-T_{16})/R_{18v16}$$
$$(T_{17}-T_{19})/R_{17v19}+(T_{18}-T_{19})/R_{18v19}=(T_{19}-T_{30})/R_{19v30}$$
$$(T_{21}-T_{20})/R_{21v20}+(T_{22}-T_{20})/R_{22v20}+(T_{S5}-T_{20})/R_{16S20}+(T_{S6}-T_{20})/R_{24S23}=(T_{20}-T_{33})/R_{20v33}$$
$$P_{21}=(T_{21}-T_{20})/R_{21v20}+(T_{21}-T_{30})/R_{21v30}$$
$$P_{22}=(T_{21}-T_{20})/R_{22v20}+(T_{22}-T_{30})/R_{22v30}$$
$$T_{23}-T_{20}=0$$
$$(T_{26}-T_{24})/R_{26v24}+(T_{25}-T_{24})/R_{25v24}+(T_{S7}-T_{24})/R_{24S27}+(T_{S6}-T_{24})/R_{24S23}=(T_{24}-T_{33})/R_{24v33}$$
$$P_{25}=(T_{25}-T_{24})/R_{25v24}+(T_{25}-T_{30})/R_{25v27}$$
$$P_{26}=(T_{26}-T_{24})/R_{26v24}+(T_{26}-T_{30})/R_{26v27}$$
$$T_{27}-T_{30}=0$$
$$T_{28}=15$$
$$T_{29}=15$$

$$(T_2-T_{30})/R_{2v30}+(T_3-T_{30})/R_{3v30}+(T_7-T_{30})/R_{7v30}$$
$$+(T_{10}-T_{30})/R_{10v30}+(T_{11}-T_{30})/R_{11v30}+(T_{14}-T_{30})/R_{14v30}$$
$$+(T_{15}-T_{30})/R_{15v30}+(T_{19}-T_{30})/R_{19v30}+(T_{21}-T_{30})/R_{21v30}$$
$$+(T_{22}-T_{30})/R_{22v30}+(T_{26}-T_{30})/R_{26v30}+(T_{25}-T_{30})/R_{25v27}$$
$$+(T_{S7}-T_{30})/R_{24S27}=(T_{30}-T_{34})/R_{30v34}$$
$$(T_{33}-T_{31})/R_{33v31}=(T_{31}-T_{29})/R_{31v29}+(T_{31}-T_{34})/R_{31v34}$$
$$(T_{33}-T_{32})/R_{33v32}=(T_{32}-T_{29})/R_{32v29}+(T_{32}-T_{34})/R_{32v34}$$
$$(T_1-T_{33})/R_{1v33}+(T_4-T_{33})/R_{4v33}+(T_9-T_{33})/R_{9v33}$$
$$+(T_{13}-T_{33})/R_{13v33}+(T_{16}-T_{33})/R_{16v33}+(T_{20}-T_{33})/R_{20v33}$$
$$+(T_{24}-T_{33})/R_{24v33}=(T_{33}-T_{31})/R_{33v31}+(T_{33}-T_{32})/R_{33v32}$$
$$+(T_{33}-T_{28})/R_{33v28}$$
$$T_{34}=10$$
$$P_{S1}=(T_{S1}-T_1)/R_{1S4}+(T_{S1}-T_4)/R_{1S4}$$
$$P_{S2}=(T_{S2}-T_4)/R_{4S8}+(T_{S2}-T_9)/R_{4S8}$$
$$P_{S3}=(T_{S3}-T_9)/R_{9S12}+(T_{S3}-T_{13})/R_{9S12}$$
$$P_{S4}=(T_{S4}-T_{13})/R_{13S16}+(T_{S4}-T_{16})/R_{13S16}$$
$$P_{S5}=(T_{S5}-T_{16})/R_{16S20}+(T_{S5}-T_{20})/R_{16S20}$$
$$P_{S6}=(T_{S6}-T_{20})/R_{24S23}+(T_{S6}-T_{24})/R_{24S23}$$
$$P_{S7}=(T_{S7}-T_{24})/R_{24S27}+(T_{S7}-T_{30})/R_{24S27}$$

Through MATLAB programming, the Gauss-Seidel iteration method is used to calculate the heat production of heat source and the thermal resistance between parts. substituting it into the heat balance equation system, the temperature of each temperature node can be obtained.

D. Thermal Balance Analysis Results

The calculated values of heat generation, heat dissipation and thermal resistance of the ranging arm are substituted into the MATLAB calculation program. The temperature values of each component of the ranging arm and lubricating oil are obtained under the conditions of 0 C, 10 C, 20 C and 30 C respectively when the temperature of the ranging arm reaches the thermal balance. The outside wall of ranging arm is shown Figure 5. The temperature values of each wall of ranging arm shell and lubricant balance temperature values are extracted as shown in Table 1. Table 1 shows the thermal balance temperature of each outer wall and the oil balance temperature at different environment temperatures.

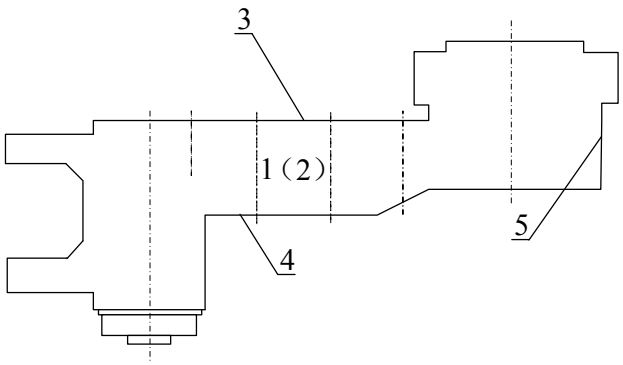

FIGURE V. SIMPLIFIED DRAWING OF OUTSIDE-WALL OF RANGING ARM

TABLE I. THERMAL BALANCE TEMPERATURE ON OUTSIDE-WALL OF RANGING ARM AND LUBRICATING OIL UNDER DIFFERENT ENVIRONMENT TEMPERATURE (UNIT: °C)

The environment temperature	Wall1	Wall 2	Wall 3	Wall 4	The Balance oil temperature
0	36.47	53.24	51.18	51.18	55.92
10	46.69	60.09	59.35	59.35	62.89
20	57.72	73.33	69.71	69.71	72.25
30	66.31	81.23	78.85	78.85	82.56

It can be seen from Table 1 that when the environment temperature is the same, the temperature of wall 1 is obviously lower than other walls, and the temperature of wall 2 is obviously higher than other walls. The main reason is that wall 1 is the upper wall of ranging shell, with large heat dissipation area and no contact with high temperature lubricating oil, while wall 2 is the lower wall of ranging shell, with small heat dissipation area and direct contact with high temperature lubricating oil. When the temperature of the lower wall is higher than the upper wall, due to the thermal expansion effect of the material, the elongation of the lower wall of the ranging arm shell will be significantly larger than the upper wall, which will increase the deformation and thermal stress of the shell. It is not conducive to the performance of the ranging arm shell and the ranging arm transmission system. Therefore, in order to solve the problem of excessive temperature difference between wall 1 and wall 2, the area and channel number of wall 2 spray water jacket can be increased without affecting the stiffness and strength of ranging shell. So as to ensure that the temperature difference between upper and lower wall of ranging shell within a reasonable range, and reduce the thermal expansion effect of material.

The environment temperature is not the same, and the wall temperature increases with the increase of environment temperature. Because the air temperature passing through the ranging arm shell surface is high when the environment temperature is high. The air motion viscosity increases, and the air convection heat transfer capacity decreases, thus reducing heat dissipation, making the ranging shell wall and the balance oil temperature higher, so the ranging arm temperature should be detected in time under the high temperature environment.

The thermal network method can be used to calculate the wall temperature and lubricant temperature of the ranging arm shell when the ranging arm reaches the thermal balance. Thermal balance analysis of the ranging arm of the drum shearer is carried out, and data support is provided for the finite element thermal analysis and thermal structure coupling analysis of the ranging arm shell.

IV. THERMODYNAMIC SIMULATION

The theory of thermal analysis and thermal structure coupling analysis has been developed very maturely and has been widely used in the machinery industry. However, there are few applications in coal mine machinery, especially the research on the ranging arm shell of shearer. In this section, the ranging arm shell is taken as the research object, and the thermal analysis and thermal structural characteristics of the ranging arm shell are analyzed.

A. Thermal Analysis

The thermal load affecting the temperature distribution of the ranging arm shell mainly includes two types. One is the thermal load that causes the ranging arm to heat up, that is the heat generated by the rotation of the bearing, the heat transfer of the lubricating oil and the ranging arm shell, the oil and gas and the wall surface of the ranging arm shell. The other is the thermal load that causes the ranging arm shell to cool down, that is the heat transfer between the spray cooling system and the ranging arm shell, and the heat convection between the air and the ranging arm housing. The ranging arm shell is integrally cast and the material is cast steel. The material properties are shown in Table 2. Applying the relevant temperature parameters calculated in the previous section to the simplified ranging arm shell, the temperature distribution map of the ranging arm shell is shown in Figure 6.

TABLE II. MATERIAL PROPERTIES OF RANGING ARM HOUSING

Modulus of elasticity (Pa)	Poisson 's ratio	Density (kg/m^3)	Specific heat capacity (J/kg·K)	Thermal conductivity (W/m·K)	Thermal expansion coefficient (K)
1.75E11	0.3	7800	460.5	31	10E-6

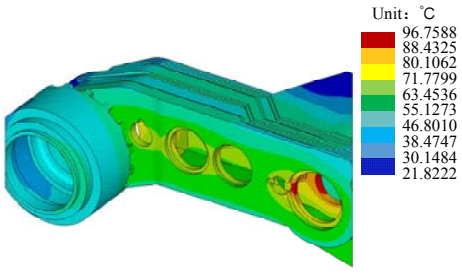

FIGURE VI. TEMPERATURE FIELD DISTRIBUTION OF RANGING ARM

It can be seen from Figure 5 that the temperature range of the ranging arm shell is between 21.822°C and 96.758°C, the temperature distribution on the outer wall surface of the coal wall side is relatively uniform, and the upper wall surface is relatively low in temperature due to the provision of a cooling water jacket. The temperature is significantly lower than the temperature of the sidewall of the ranging arm shell. The highest temperature appears between the bearing hole of the ranging arm shell and the bearing hole of the idler bearing, and the temperature value is 96.758 °C.

B. Thermal-structural Coupling Analysis

The stress and deformation of the ranging shell under static loading and cutting load and torque are obtained as shown in Figure 7. Thermal steady state analysis is carried out on the basis of the stress and deformation. Thermal analysis results are loaded into the static analysis Thermal structure coupling analysis results of the ranging shell are shown in Figure 8 and Figure 9.

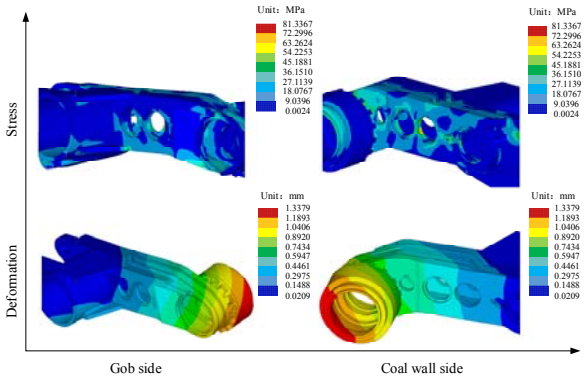

FIGURE VII. STRESS AND DEFORMATION DISTRIBUTION OF RANGING ARM HOUSING UNDER ALL LOAD

It can be seen from Figure 8 that the maximum stress is 105.79 MPa at the joint of the traction portion. The maximum stress of the ranging shell is 85.76 MPa without the temperature, and the maximum stress position is different. This indicates that the temperature affects the ranging arm. The shell stress distribution and the maximum stress value increased by 30.3%.

According to Figure 9, the maximum deformation is at the inner ring gear connected to the ranging arm housing, and the value is 2.59 mm. Compared with Figure 6, the position of maximum displacement is the same in both cases, mainly because the ranging shell is similar to the cantilever beam model, and the free end will have relatively large deformation after loading. The maximum deformation of ranging arm shell is 1.57 mm without considering the influence of temperature field. The maximum deformation of ranging arm shell is increased by 94.7% due to temperature field. Therefore, the distribution of temperature field has an important influence on the deformation of ranging arm shell.

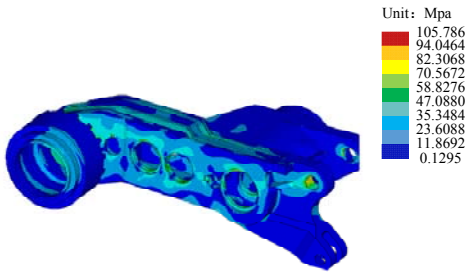

FIGURE VIII. THERMAL STRUCTURAL COUPLING STRESS OF RANGING ARM HOUSING

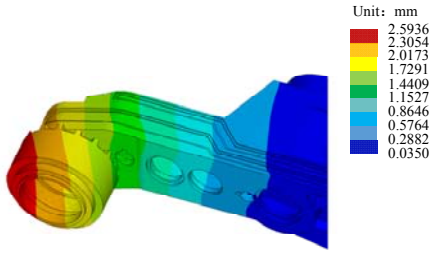

FIGURE IX. THERMAL STRUCTURAL COUPLING DEFORMATION OF RANGING ARM HOUSING

V. EXPERIMENT

According to the loading test requirement and data acquisition requirement of shearer ranging arm, the loading test system is designed as shown in Figure 10. The test system is composed of measured parts, temperature measuring device, dynamometer, signal acquisition and transmission system, etc. In this experiment, only the ranging arm is applied with torque to measure the temperature field distribution and stress change of the ranging arm shell under the action of torque. The infrared thermometer is used to monitor the temperature of the ranging arm during the loading process of the ranging arm. A strain gauge is attached to the ranging arm housing to test the stress of the ranging arm shell under the stress and heat balance temperature of the casing at ambient temperature. Compare the stress levels at two different temperatures. The ranging loading test is completed after the ranging arm reaches the balance temperature.

The finite element steady state thermal analysis of the ranging arm shell was used to compare the temperature of the coal wall side, the bearing hole node of the gob side， the upper and lower wall surfaces, and compared with the heat balance temperature of the ranging arm shell obtained in the ranging loading test. The result is shown in Figure. 11. and Figure 12.

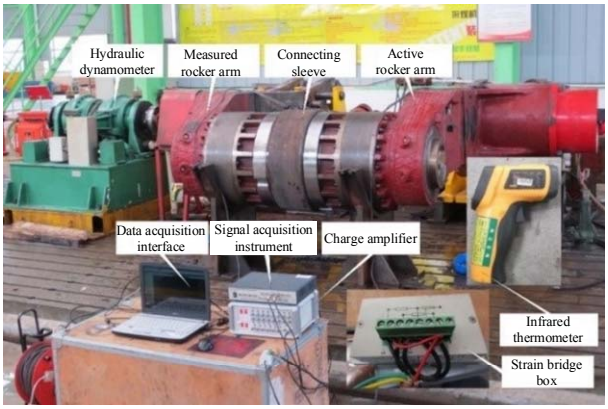

FIGURE X. FLOADING TEST-SYSTEM FOR RANGING ARM

It can be seen from analysis of Figure 11 and Figure 12 that the simulation temperature value of different measuring points on the ranging arm casing are consistent with the test temperature values. This shows that the temperature field distribution obtained by the finite element analysis of the ranging arm shell is basically consistent with the test temperature field distribution. Comparing the finite element temperature value of each temperature measurement point with the test temperature value, it is known that the test temperature values of all other measurement points are larger than the finite element analysis value except for a few points. The maximum error rate is about 16.9%, and the average error of each measuring point is 10.3%, which indicates that the mathematical model and finite element simulation calculation method of the ranging arm heat and heat dissipation used in this paper are basically correct.

In order to study the influence of the temperature field on the stress of the ranging shell, the strain gauges were used to measure the stress values of the idle shaft hole of the ranging shell under ambient temperature and heat balance temperature.

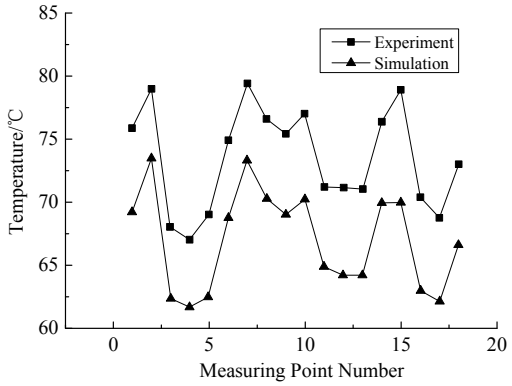

(a)Coal wall side

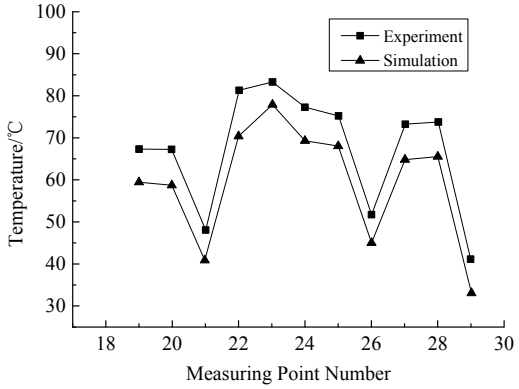

(b)Gob side

FIGURE XI. COMPARISON BETWEEN EXPERIMENT AND SIMULATION TEMPERATURE ON COAL WALL AND GOB OF THE RANGING ARM SHELL

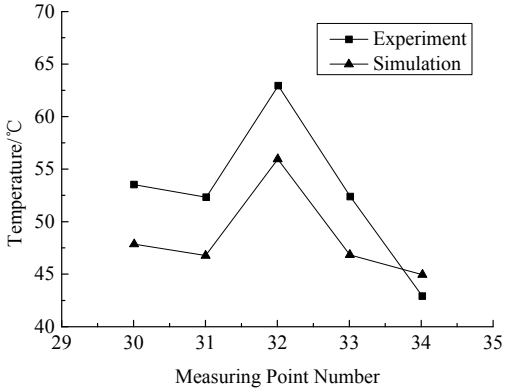

(a)Upper wall surface

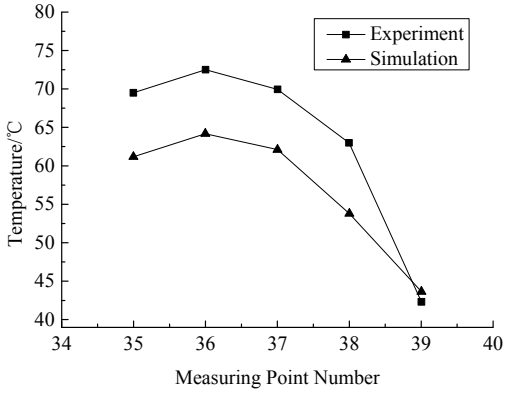

(b)Inferior wall surface

FIGURE XII. COMPARISON BETWEEN EXPERIMENT AND SIMULATION TEMPERATURE ON THE TOP WALL AND THE BOTTOM WALL OF THE RANGING ARM SHELL

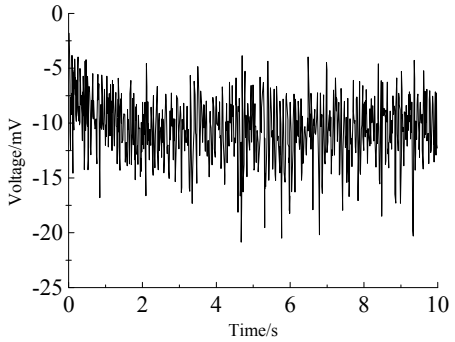

FIGURE XIII. OUTPUT VOLTAGE SIGNAL VARIATION CURVE OF STRESS UNDER AMBIENT TEMPERATURE

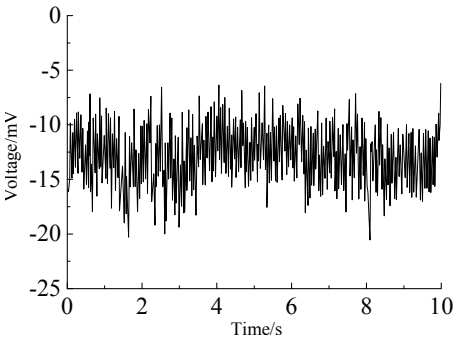

FIGURE XIV. OUTPUT VOLTAGE SIGNAL VARIATION CURVE OF STRESS UNDER THERMAL EQUILIBRIUM TEMPERATURE

Loading the ranging arm on the test bench and measuring the stress at the strain gauge attached to the idle shaft hole at ambient temperature and heat balance temperature. It can be seen from Figure 13 and Figure 14 that the output of the voltage signal at the strain gauge of the idle shaft hole is kept substantially constant at an ambient temperature, the average voltage is 10.5 mV, and the finite element simulation value of the stress measurement point is 6.3 MPa. After the ranging arm reaches the heat balance, the temperature of the casing rises, and the stress at the position of the idle shaft of the ranging arm shell is kept constant, the average voltage is 12.8 mV, and the finite element simulation value of the stress measurement point is 7.6 MPa. The results show that considering the influence of the heat balance temperature field, the stress at the position measured by the ranging arm shell increases by 14.7%. According to the finite element value of the position measured by the ranging arm shell, the measured position stress at the heat balance temperature is 21.9% higher than the ranging arm stress at ambient temperature. Compared with the experimental results, the stress variation error of the measuring point in the finite element calculation is 7.2%.

VI. CONCLUSION

In this paper, the ranging arm shell of the drum shearer is taken as the research object. The mechanical properties, temperature field distribution and thermal structure characteristics of the ranging shell are analyzed by the

combination of theoretical calculation, simulation analysis and experimental research. The following conclusions are drawn:

1) The simulation results of the thermal structure coupling of the ranging arm shell show that the maximum stress and maximum deformation of the ranging arm shell are significantly increased considering the thermal equilibrium temperature field distribution.

2) The test results of the wall temperature field and the ranging shell stress show that the analysis results of the rock-arm shell thermal coupling model established in this paper can better reflect the shell stress variation law in the actual working process. The rationality of the heat generation and heat dissipation factors of the shearer ranging analyzed in this paper and the correctness of the established mathematical model of heat balance are verified.

ACKNOWLEDGMENTS

This research is supported by Tiandi Science & Technology Co, Ltd.'s Science and Technology Innovation Venture Capital Project (2018-TD-ZD009).

REFERENCES

[1] Gao H B, Sun N, Zhang R Q, et al. DynamicAnalysis and Study on Shaft's Torsional Vibration of Electrical Traction Shearer's Motor-Ranging and Deceleration System[C]//2009 Second International Conference on Intelligent Computation Technology and Automation. IEEE, 2009, 3:54-57.

[2] Si L, Wang Z, Liu X, et al. Cutting state diagnosis for shearer through the vibration of ranging transmission part with an improved probabilistic neural network[J]. Sensors, 2016, 16(4): 479.

[3] Jianjian Y, Ran X, Di L, et al. Analysis of sh-earer gear vibration in the no-load state[C]//2013 Fifth International Conference on Measuring Technology and Mechatronics Automation. IEEE, 2013: 247-250.

[4] Zhi-peng X, Zhong-bin W. Modelling and simulation on shearer self-adaptive memory cutting[J]. Procedia Engineering, 2012, 37: 37-41.

[5] Wan L, Wang Z, Meng Z, et al. Static Analysis and Improvement of Ranging Arm of Shearer Based on ANSYS[C]//2015 6th International Conference on Manufacturing Science and Engineering. Atlantis Press, 2015.

[6] LIAN Z, LIU K. Virtual prototype of shearer ranging arm and its dynamics analysis [J]. Journal of China Coal Society,2005(06):801-804.(In Chinese)

[7] Zhang Y, Huang J, Zhu L, et al. Reliability-based robust optimization design of the transmission system of a shearer ranging arm[J]. Journal of China Coal Society, 2015, 40(11):2540－2545. (In Chinese)

[8] Mao J, Zhu Y, Chen H, et al. Gear solid-heat coupled analysis and tooth profile modification of ranging arm of shearer[J]. Journal of China Coal Society, 2017, 42(6):1598－1606. (In Chinese)

[9] Chen J, Li W, Xin G, et al. Nonlinear dynamic characteristics analysis and chaos control of a gear transmission system in a shearer under temperature effects[J]. Proceedings of the Institution of Mechanical Engineers, Part C: Journal of Mechanical Engineering Science, 2019: 0954406219854112.

[10] CHEN Hongyue, LI Yuzhu, ZHANG Zhao, et al. Analysis of solid-thermal-mechanical coupling characteristics of ranging-arm gear drive system of shearer[J]. Journal of China Coal Society, 2018, 43(3) :878－887. (In Chinese)

[11] HARRIS T A. Rolling bering anaylsis[M].New York: JOHN WIEYANDSONS,INC,1990.

[12] Yasutsune Arirua, The lubricant churing loss in spur gear system[J].Bullentin of the JSME,1973.16(95):126-139.

[13] Yang S, Tao W. Third Edition of Heat Transfer [M].Beijing : Higher Education Press, 1998. (In Chinese)

[14] Huang Z. Investigation on Thermo Balance of Transmission Gearbox in High Speed Train[D].Shanghai : Shan-ghai Jiaotong University, 2007. (In Chinese)

[15] Zhang X.Thermal and Structural Characteristic Analysis and Research of Case for Wind Turbine Generator Gearbox[D].Dalian : Dalian University of Technology, 2009. (In Chinese)

[16] Deng C.Heat balance Analysis and Simulation of a Mechanical[D].Changchun : Jilin University, 2007.

[17] Beatriz Lopez-Walle. Dynmic modeling for thermal micro-actuators using thermal networks[J].Internatonal Journal of Thermal Sciences[J].2010,11:2109-2116. (In Chinese)

[18] Xu Z. Thermal analysis of the shearing system of the shearer [D].Xuzhou: China University of Mining and Technology, 2009. (In Chinese)